NASA TECHNICAL MEMORANDUM

NASA TM X-71593

NASA TM X-71593

QUASI-THREE-DIMENSIONAL FLOW SOLUTION BY MERIDIONAL PLANE ANALYSIS

by Theodore Katsanis and William D. McNally
Lewis Research Center
Cleveland, Ohio 44135

TECHNICAL PAPER proposed for presentation at National Aerospace Engineering Meeting sponsored by the Society of Automotive Engineers San Diego, California, September 30-October 4, 1974

QUASI-THREE-DIMENSIONAL FLOW SOLUTION BY MERIDIONAL PLANE ANALYSIS

by Theodore Katsanis and William D. McNally

Lewis Research Center

E-8048

ABSTRACT

A computer program has been developed to obtain subsonic or shock-free transonic, nonviscous flow analysis on the hub-shroud mid-channel flow surface of a turbomachine. The analysis may be for any annular passage, with or without blades. The blades may be fixed or rotating and may be twisted and leaned. The flow may be axial, radial or mixed.

Blade surface velocities over the entire blade are approximated based on the rate of change of angular momentum. This gives a 3-D flow picture based on a 2-D analysis.

The paper discusses the method used for the program and shows examples of the type of passages and blade rows which can be analyzed. Also, some numerical examples are given to show how the program can be used for practical assistance in design of blading, annular passages, and annular diffusers.

INTRODUCTION

The design of blades for compressors and turbines ideally requires analysis methods which include unsteady, rotational, three-dimensional, and viscous effects. Clearly, such solutions are impractical at the present time, even on the largest and fastest computers. The usual approach at present is to analyze only steady flows and to separate inviscid solutions from viscous solutions. At present, inviscid analyses usually involve a combination of two-dimensional solutions on intersecting families of stream surfaces to obtain what is called a quasi-three-dimensional solution.

Since there are several choices of two-dimensional surfaces to analyze, and many ways of combining them, there are many approaches to obtaining a quasi-three-dimensional solution. Most two-dimensional solutions are either on a blade-to-blade surface of revolution (Wu's S_1 surface, (1)*, see fig. 1) or on the mid-channel stream surface between two blades (Wu's S_2 surface). Another type of two-dimensional solution can be obtained on a passage cross-sectional surface (normal to the flow).

In this paper a solution to the equations of flow on the mid-channel S_2 surface is presented. This solution surface is chosen when the turbomachine under consideration has significant variation in flow properties in the hub-shroud direction. A solution on the mid-channel surface will show this variation. The solution can be obtained either by the quasi-orthogonal method, which solves the velocity-gradient equation from hub to shroud on the mid-channel flow surface (2), or by a finite-difference method, which solves a finite-difference equation for stream function on the same flow surface. The quasi-orthogonal method is efficient in many cases and can obtain solutions into the transonic regime. However, there is a convergence problem when aspect ratios are above 1 or when the passage has high wall curvature compared to the passage height. For such cases, the most promising method is the finite-difference solution, but this solution is limited to completely subsonic flows.

The method described in this paper uses the finite-difference method, followed by velocity gradient method, if necessary. When there is transonic flow, the finite difference method is used to obtain a reduced mass flow subsonic solution for flow angles and streamline curvatures. This

*Numbers in parentheses designate references at end of paper.

information is then used with the velocity gradient method to obtain the transonic solution.

A computer program, MERIDL, has been written to perform these calculations (3 and 4). This program is written for axial-, radial-, or mixed-flow in any annular passage, with or without blades. Upstream and downstream flow conditions can vary from hub to shroud. The solution is for compressible, shock-free flow, or incompressible flow. Provision is made for an approximate correction for loss of stagnation pressure through the blade row. The blade row may be either fixed or rotating and may be twisted and leaned. The blades can have high aspect ratio and arbitrary thickness distribution.

The solution obtained by this program also provides the information necessary for a more detailed flow analysis on blade-to-blade surfaces (fig. 1). A useful program for this purpose is TSONIC (5). Information needed to prepare all the input for TSONIC is calculated and printed by MERIDL.

To give an idea of the type of problem that can be anlyzed with MERIDL, a few illustrations are given. The first illustration is an axial compressor blade row with high aspect ratio and high twist, shown in figure 2.

Another type of problem is shown in figure 3. The entire annular passage here could be analyzed as 4 cases. First, is the inlet mixed flow bladeless passage, second the axial stator, third the axial rotor, and finally the mixed flow diffuser. There can be whirl in the ducts, and the whirl, temperature and stagnation pressure can vary from hub to shroud. Each of the 4 cases would be analyzed separately, and each case would have to be matched to the adjacent case.

Figure 4 shows another row type where this method applies. This is

a radial turbine. The stator and rotor would be analyzed separately. Since this stator would be expected to have uniform flow from hub to shroud, it could best be analyzed by a blade-to-blade program such as TSONIC (5). The rotor could be analyzed with MERIDL. The rotor could have either radial of swept blades. MERIDL has not been coded to analyze a case with splitter blades.

This paper describes the MERIDL program computer requirements and the computer input and output. The method of analysis is explained briefly, with a list of the basic assumptions. Finally, three numerical examples are given to show the results that can be obtained.

COMPUTER PROGRAM

The computer program MERIDL has been implemented on the NASA Lewis time sharing IBM-TSS/360-67 computer as well as the NASA Lewis Univac 1106 computer. Storage for program variables requires 60,000 words for a 41-axial by 21-radial grid; storage for the program code is 18,000 words additional. Run times range from 3 to 15 minutes on the IBM 360-67 equipment, depending upon the mesh size used and the compressibility of the flow. The MERIDL program is available through COSMIC at the University of Georgia, and is documented thoroughly in (3 and 4).

Input to the program consists primarily of blade section and hub-shroud geometry as well as upstream and downstream flow-variable boundary conditions. The major input is summarized on figure 5. Hub and shroud geometries are both given by z vs. r spline coordinates. Blade geometry is described by a series of blade sections from hub to shroud on blade-to-blade surfaces of revolution. Meanline (θ) and blade thickness coordinates are given as functions of z and r to define these blade sections. Upstream and downstream flow boundary conditions are given at a number of locations from hub to shroud. Upstream of the blade row, total tem-

perature, total pressure, and inlet whirl (tangential velocity) are required, while downstream total pressure (or loss) and outlet whirl are given. These conditions, along with mass flow, define the inviscid problem to be solved.

Output from the program can be obtained at any points within the solution region at which it is requested by the user. Ordinarily output is requested along user-designated streamlines, the locations of which are calculated by the program. It can also be obtained on the finite-difference solution mesh. Output is calculated after each major iteration of the solution and after any velocity gradient solutions. The user can control the number of iterations at which he desires it to be printed. Figure 6 shows the most important output which usually requested.

There are many types of output which can be given, but the most common variables printed at a requested set of points are the following:

Streamline Coordinates . . . . . z, r
Meridional Velocity . . . . . W_m
Tangential Velocity . . . . . W_θ
Relative Velocity . . . . . W
Meridional Flow Angle . . . . . α
Blade-to-Blade Flow Angle . . . . . β
Critical Velocity Ratio . . . . . W/W_{cr}
Streamline Curvature
Blade Surface Velocities . . . . . W_l, W_{tr} (within blade regions)

See figure 7 and the list of Symbols for the definition of these variables. Extensive plots can also be obtained of both the geometrical and fluid input variables and of the major output variables. The principal outputs plotted are the calculated streamline pattern in the meridional plane as well as meridional and blade surface velocities along these streamlines.

When a reasonable flow pattern has been achieved by MERIDL on the mid-channel flow surface, more detailed and accurate blade surface veloc-

ities can be obtained on blade-to-blade surfaces which follow the direction of the calculated meridional streamlines. Several blade elements or stream channels can be analyzed from hub to shroud using the TSONIC program (5) to build a quasi-three-dimensional solution for the full flow passage. MERIDL calculates and prints most of the input required for the TSONIC blade-to-blade program along each of the calculated stream channels (fig. 6).

METHOD OF ANALYSIS

BASIC ASSUMPTIONS - It is desired to determine the flow distribution through an annular duct, or through a stationary or rotating cascade of blades on a mid-channel hub-shroud stream surface. The following simplifying assumptions are used in deriving the equations and in obtaining a solution:

(1) The flow relative to a blade is steady.

(2) The flow is axi-symmetric where there is no blade.

(3) The fluid is a perfect gas with constant specific heat C_p.

(4) The fluid is a nonviscous gas.

(5) There is no heat transfer.

(6) The mid-channel surface is a stream surface which has the same shape as the blade mean camber surface, except near the leading and trailing edges, where an arbitrary correction is made to match the free-stream flow.

(7) The only forces are those due to momentum and pressure gradient.

(8) The velocity varies linearly between blade surfaces.

(9) The relative stagnation pressure loss is known through the blade row.

The flow may be axial, mixed, or radial. There may be a variation of whirl, stagnation pressure, and stagnation temperature from hub to shroud, both upstream and downstream of the blade row. The blade row may be either fixed or rotating, with leaned and twisted blades. Within the given assumptions, no terms are omitted from the equations.

SOLUTION BY COMBINATION OF METHODS - A flow analysis on the meridional flow surface can be obtained either by the velocity-gradient method or by the finite-difference method. The finite-difference solution of the stream function equation is limited to subsonic flow, whereas the velocity-gradient method by itself is limited to relatively low-aspect-ratio blades. Of these two methods the most accurate solution is obtained by the finite-difference technique, so that this method is used where possible (i. e., for subsonic flow). In cases which have locally supersonic flow, the finite-difference solution is first obtained at a reduced mass flow for which the flow field is completely subsonic. The streamline curvatures and flow angles throughout the passage which are obtained from this solution provide the information necessary to obtain an approximate velocity-gradient solution at full mass flow, even with high aspect ratio and high wall curvature.

SUBSONIC STREAM-FUNCTION SOLUTION - The stream-function equation is a partial differential equation on a mid-channel hub-shroud stream surface (see assumption 6). This equation is in one unknown (the stream function u) as a function of two variables, r and z (see fig. 7).

$$\left.\begin{aligned} &\frac{\partial^2 u}{\partial z^2} + \frac{\partial^2 u}{\partial r^2} - \frac{1}{r}\frac{\partial u}{\partial r} - \left(\frac{1}{B}\nabla B + \frac{1}{\rho}\nabla\rho\right)\cdot\nabla u + \frac{rB\rho}{wW_z}\left[\frac{W_\theta}{r}\frac{\partial(rV_\theta)}{\partial r} + \xi W^2 + \zeta + F_r\right] = 0 \\ &\text{where} \\ &\xi = \frac{1}{2C_p}\left(\frac{R}{p''}\frac{\partial p''}{\partial r} - \frac{1}{T''}\frac{\partial I}{\partial r} - \frac{\omega^2 r}{T''}\right) \\ &\zeta = \omega^2 r - \frac{RT''}{p''}\frac{\partial p''}{\partial r} \\ &F_r = \frac{\partial\theta}{\partial r}\frac{1}{\rho}\frac{\partial p}{\partial\theta} \end{aligned}\right\} \quad (1)$$

The derivatives of the stream function satisfy the equations

$$\left.\begin{aligned} \frac{\partial u}{\partial z} &= -\frac{rB\rho W_r}{w} \\ \frac{\partial u}{\partial r} &= \frac{rB\rho W_z}{w} \end{aligned}\right\} \tag{2}$$

Equation (1) is derived from Wu's equation (eq. (107a), (1)) for the stream function on what he calls an S_2 surface. Equation (1) is nonlinear but can be solved iteratively by the finite-difference method when the flow is completely subsonic.

A finite region (as indicated in fig. 8) is considered for the solution of equation (1). It is assumed that the upstream and downstream boundaries are sufficiently far from the blade so as to have a negligible effect on the solution. Equation (1) is elliptic for subsonic flow. Therefore, when the flow is entirely subsonic, equation (1) can be solved when proper boundary conditions are specified on the entire boundary of the region. These conditions are the values of the stream function on all four boundaries. The stream function has the value 0 on the hub and 1 at the shroud. The value of the stream function on the upstream and downstream boundaries can be calculated if the stagnation pressure, stagnation temperature, and whirl distribution from hub to shroud are specified upstream and downstream of the blade.

The numerical solution of equation (1) is obtained by the finite-difference method. The finite-difference grid is an orthogonal mesh which is generated by the program, using the method reported in reference (6). Figure 9 illustrates the orthogonal finite-difference mesh.

The finite-difference equations are nonlinear since the original equation (1) is nonlinear. These equations can be solved iteratively. On the first iteration an initial density is assumed; this linearizes some of the

terms. The remaining nonlinear terms are omitted for the first iteration so that the finite-difference equations are entirely linearized. These linearized equations are then solved to obtain the first approximate solution for stream function. This solution provides information used to obtain a better estimate of the density and an estimate of the other nonlinear terms. The equations are the solved again to obtain an improved solution. This process is repeated, and by iteration a final converged solution can be obtained if the flow is subsonic.

For each step of this iteration, the linearized finite-difference equations must be solved. The method used to solve the equations is successive overrelaxation (8) with an optimum overrelaxation factor. Since this is also an iterative method, we have two levels of iteration.

After the stream function is obtained, the velocity distribution is obtained by numerical partial differentiation of the stream function and by using equation (2). The details of the numerical procedure and programming technique are described in reference (4).

TRANSONIC VELOCITY-GRADIENT APPROXIMATE SOLUTION - For the case where there is locally supersonic flow, equation (1) is no longer elliptic in the entire region but is hyperbolic in the region of supersonic flow (7). This changes the boundary conditions and means that there will probably be shock losses in going from supersonic to subsonic flow. The finite-difference method cannot be used with locally supersonic flow. However, an approximate solution can be obtained by getting a reduced-flow solution with the finite-difference method and extending this to the full flow by using the velocity-gradient method. This technique is described in reference (5).

The velocity-gradient equation is

$$dW = \left(aW + b + \frac{c}{W} + d\cos\beta\right) dt + \frac{e}{W} + Wf \cdot \tag{3}$$

The coefficients, a, b, c, and d, are given by different expressions in the blade region, in the upstream region, and in the downstream region. These coefficients are given as follows:

Blade region coefficients:

$$\left.\begin{aligned} a &= \frac{\cos^2\beta\cos(\alpha - \varphi)}{r_c} - \frac{\sin^2\beta\cos\varphi}{r} + \sin\alpha\sin\beta\cos\beta\frac{\partial\theta}{\partial t} \\ b &= \cos\beta\frac{dW_m}{dm}\sin(\alpha - \varphi) - 2\omega\sin\beta\cos\varphi + r\cos\beta\left(\frac{dW_\theta}{dm} + 2\omega\sin\alpha\right)\frac{\partial\theta}{\partial t} \\ c &= 0 \\ d &= 0 \end{aligned}\right\} \tag{4}$$

Upstream-region coefficients:

$$\left.\begin{aligned} a &= \frac{\cos(\alpha - \varphi)}{r_c} \\ b &= 0 \\ c &= -\left(\frac{\lambda - \omega r^2}{r^2}\right)\left[\frac{\lambda - \omega r^2}{r_c}\cos(\alpha - \varphi) + \frac{\lambda + \omega r^2}{r}\cos\varphi\right] \\ d &= \frac{dW_m}{dm}\sin(\alpha - \varphi) \end{aligned}\right\} \tag{5}$$

Downstream-region coefficients:

$$\left.\begin{aligned} a &= \frac{\cos(\alpha - \varphi)}{r_c} \\ b &= 0 \\ c &= -\left[\frac{(rV_\theta)_o - \omega r^2}{r^2}\right]\left[\frac{(rV_\theta)_o - \omega r^2}{r_c}\cos(\alpha - \varphi) + \frac{(rV_\theta)_o + \omega r^2}{r}\cos\varphi\right] \\ d &= \frac{dW_m}{dm}\sin(\alpha - \varphi) \end{aligned}\right\} \quad (6)$$

Finally, in all three regions, we have

$$\left.\begin{aligned} e &= C_p T_i' - \omega\, d\lambda - C_p dT'' + \frac{RT''}{p''}dp'' \\ f &= -\frac{R dp''}{2C_p p''} + \frac{dT''}{2T''} \end{aligned}\right\} \quad (7)$$

Equations (3) to (7) are derived in reference (3). Equation (3) is solved as an initial-value problem, where the initial value of W is specified at the hub for any given mesh line running from hub to tip. By finding several solutions for varying values of W at the hub, a solution satisfying continuity will be found; that is, the solution will satisfy

$$\int \rho W\, rB \cos(\alpha - \varphi) \cos\beta\, dt = w \quad (8)$$

When equation (3) has been solved, subject to satisfying equation (8), for every hub-to-tip mesh line in the region, the entire velocity distribution is obtained.

BLADE SURFACE VELOCITIES - The solution which is obtained by

either the finite-difference or velocity-gradient method is for the mid-channel surface between the blades. Of greater interest are the blade surface velocities from which boundary layer growth and losses can be calculated. Blade surface velocities can be estimated from the mid-channel solution since the blade loading is dependent on the rate of change of whirl. Blade surface velocities can be calculated by assuming a linear variation of velocity between blade surfaces. In reference (3) the following equation for calculating blade surface velocities is derived:

$$\left.\begin{aligned} W_l &= W_{mid} - \frac{B}{2} \cos \beta \frac{d(rV_\theta)}{dm} \\ W_{tr} &= W_{mid} + \frac{B}{2} \cos \beta \frac{d(rV_\theta)}{dm} \end{aligned}\right\} \tag{9}$$

NUMERICAL EXAMPLES

AXIAL-FLOW COMPRESSOR ROTOR - Flow was analyzed on the mid-channel flow surface of an axial-flow rotor designed with the computer program of (9). The design pressure ratio is 1.275; the inlet hub-tip radius ratio, 0.5; the aspect ratio, 1.5; the tip solidity, 1.0; and the tip relative Mach number at the inlet, 0.9. Although tip relative Mach number is near sonic, there are no locally supersonic regions on the meridional flow surface. This permitted the calculation and comparison of both the finite difference and velocity gradient solutions.

Figures 10, 11, and 12 show plots from MERIDL for this example. Figure 10 shows the input hub, shroud, and blade leading and trailing edges in the meridional plane. Design blade sections are also indicated. There were 861 mesh points: 41 in the axial direction and 21 in the radial direction. The input hub, mean and tip blade sections are shown in figure 11.

Calculated mid-channel and surface velocities obtained from MERIDL are shown in figure 12 for the hub, 50 percent, and tip streamlines.

A comparison, for the mid-channel velocities only, between the stream-function solution and the more approximate velocity gradient solution for the same weight flow is also shown on figure 12. The dashed-line velocity gradient solutions deviate very little from the stream function solution, and only do so in the blade regions where maximum turning is taking place.

More details on this example, including both input and output, are given in (3).

AXIAL-TO-RADIAL DIFFUSER DUCT - This duct is the diffuser for an axial flow turbine. Because of space limitation the flow was turned to the radial direction in a short distance. The flow angle β varies from 15° at the hub to 10° at the shroud, at the turbine rotor exit. The maximum Mach number is less than 0.4, so that the flow is fully subsonic.

Figure 13 shows the inner and outer walls of the diffuser, with the input spline points marked. There were 400 mesh points; 25 along hub and shroud and 16 across the passage from hub to shroud, as shown in figure 14. The streamlines obtained by the MERIDL finite-difference solution for increments of 10 percent flow are shown in figure 15. The velocity distribution at the inner wall, 50 percent streamline, and outer wall are shown in figure 16. The static pressure distribution along the inner and outer walls, as a function of the true streamline distance (not meridional distance) are shown in figure 17. These can be used in a boundary layer analysis to locate possible separation points.

FLARED AXIAL STATOR - This example is a stator for one stage of a multi-stage axial turbine. The hub, shroud, and blade leading and trailing edges are shown in figure 18. The blade sections at hub, mean, and tip

are shown in figure 19.

There is constant whirl entering the blade row. Because of the curvature and change of radius of the hub and shroud, the whirl angle changes rapidly just ahead of the blade leading edge. Small changes in hub or shroud change these flow angles drastically, which can lead to large incidence losses. The MERIDL finite-difference solution was used to calculate the flow angle just ahead of leading edge for several hub and shroud contours. The flow angles for the final configuration (fig. 18) are compared with the blade angles in figure 20.

SYMBOLS

a coefficient in velocity-gradient equation (3)

B tangential space between blades, rad

b coefficient in velocity-gradient equation (3)

C_p specific heat at constant pressure, J/(kg) (K)

c coefficient in velocity-gradient equation (3)

d coefficient in velocity-gradient equation (3)

e coefficient in velocity-gradient equation (3)

F vector normal to mid-channel stream surface and proportional to tangential pressure gradient, N/kg

f coefficient in velocity-gradient equation (3)

l rothalpy, $C_p T_i' - \omega\lambda$, meters^2/sec^2

m meridional streamline distance, meters

p pressure, N/meters^2

R gas constant, J/(kg) (K)

r radius from axis of rotation, meters

r_c radius of curvature of meridional streamline, meters

T temperature, K

t distance along orthogonal mesh lines in direction across flow

u normalized stream function

W fluid velocity relative to blade, meters/sec

w mass flow, kg/sec

z axial coordinate, meters

α angle betweem meridional streamline and axis of rotation, rad; see figure 7

β angle between relative velocity vector and meridional plane, rad; see figure 7

ζ coefficient in stream-function equation, defined in equation (1)

θ relative angular coordinate, rad; see figure 7

λ prerotation, $(rV_\theta)_i$, meters^2/sec

ξ coefficient in stream-function equation, defined in equation (1)

ρ density, kg/meter^3

φ angle between s-coordinate line and axis of rotation, rad; see figure 4

ω rotational speed, rad/sec; see figure 7

Subscripts:

cr critical

i inlet

l blade surface facing direction of positive rotation

m component in direction of meridional streamline

mid mid-channel blade to blade

o outlet

r component in radial direction

tr blade surface facing direction of negative rotation

θ component in tangential direction

Superscripts:

' absolute stagnation condition

'' relative stagnation condition

REFERENCES

1. C. H. Wu, "A General Theory of Three-Dimensional Flow in Subsonic and Supersonic Turbomachines of Axial-, Radial-, or Mixed-Flow Types." National Advisory Committee for Aeronautics, TN 2604, Jan. 1952.

2. T. Katsanis, "Use of Arbitrary Quasi-Orthogonals for Calculating Flow Distribution in the Meridional Plane of A Turbomachine." National Aeronautics and Space Administration, TN D-2546, Dec. 1964.

3. T. Katsanis and W. D. McNally, "FORTRAN Program for Calculating Velocities and Streamlines on the Hub-Shroud Mid-Channel Flow Surface of an Axial- or Mixed-Flow Turbomachine. I - User's Manual." National Aeronautics and Space Administration, TN D-7343, July 1973.

4. T. Katsanis and W. D. McNally, "FORTRAN Program for Calculating Velocities and Streamlines on the Hub-Shroud Mid-Channel Flow Surface of an Axial- or Mixed-Flow Turbomachine. II - Programmer's Manual." National Aeronautics and Space Administration, TN D-7344, Apr. 1974.

5. T. Katsanis, "FORTRAN Program for Calculating Transonic Velocities on A Blade-to-Blade Stream Surface of A Turbomachine." National Aeronatics and Space Administration, TN D-5427, 1969.

6. W. D. McNally, "FORTRAN Program for Generating A Two-Dimensional Orthogonal Mesh Between Two Arbitrary Boundaries." National Aeronautics and Space Administration, TN D-6766, 1972.

7. A. H. Shapiro, "The Dynamics and Thermodynamics of Compressible Fluid Flow." Vol. I, New York, N. Y.: Ronald Press Co., 1953.

8. R. S. Varga, "Matrix Iterative Analysis." Englewood Cliffs, N. J.: Prentice-Hall, 1962.

9. J. Crouse, "Computer Program for the Definition of Transonic Axial-Flow Compressor Blade Rows." National Aeronautics and Space Administration, TN D-7345, Feb. 1973.

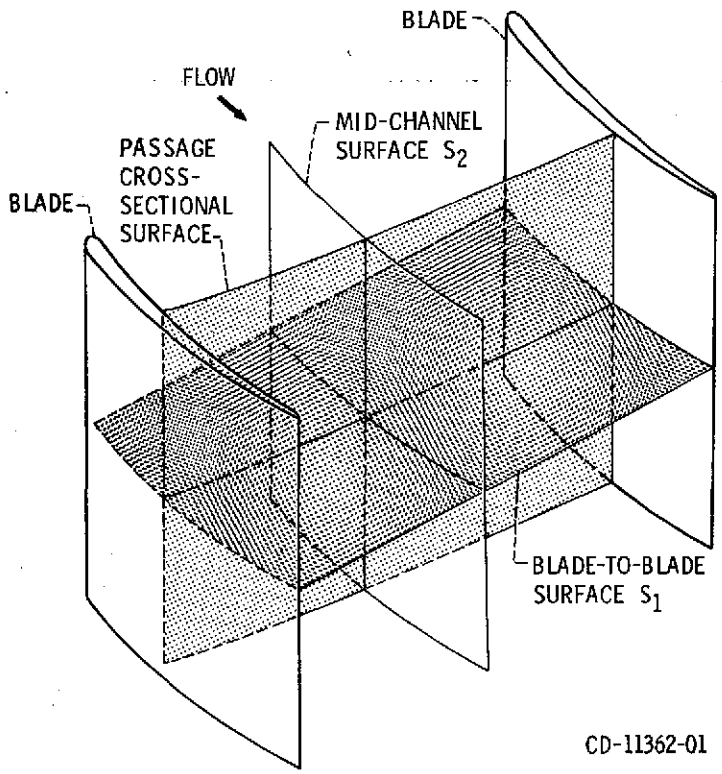

Figure 1. - Two-dimensional flow analysis surfaces.

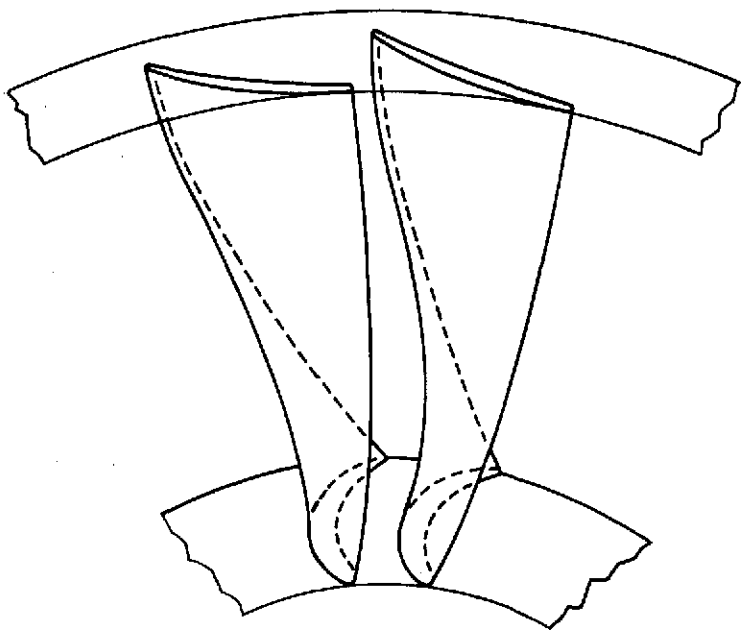

Figure 2. - Axial compressor blade row.

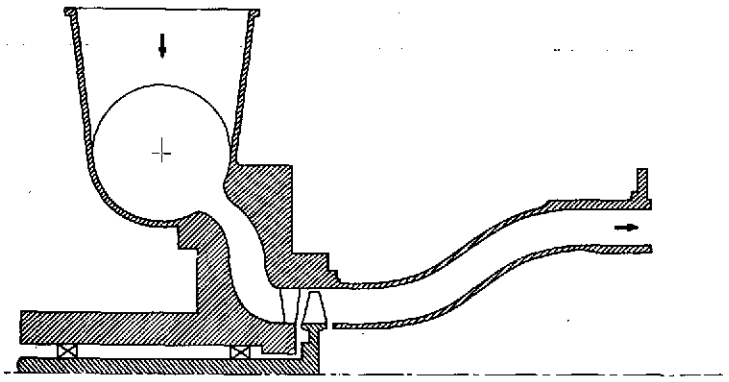

CD-9967-01

Figure 3. - Axial turbine with mixed flow annular passage.

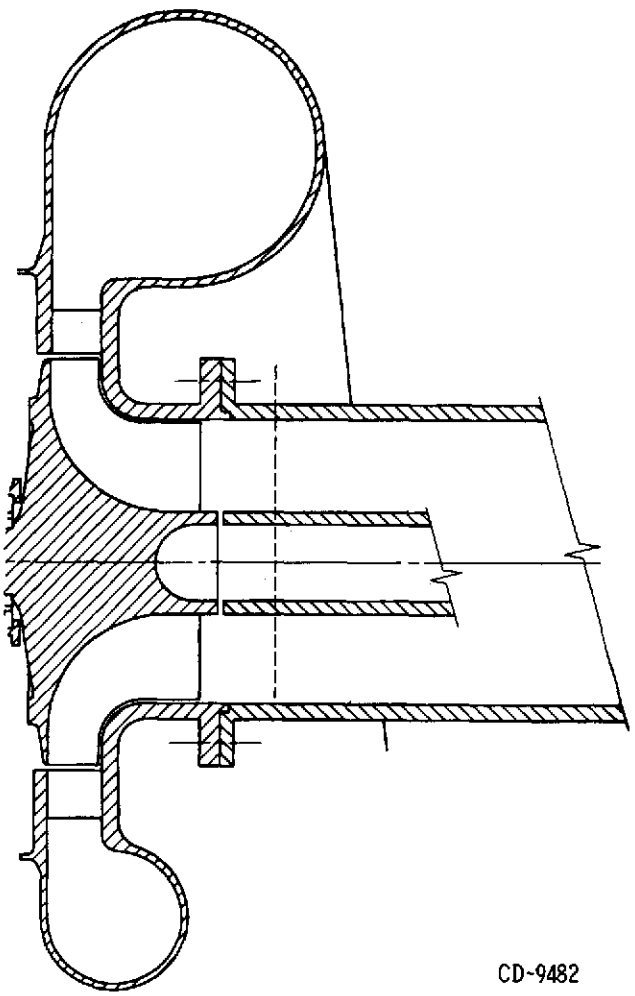

CD-9482

Figure 4. - Radial inflow turbine.

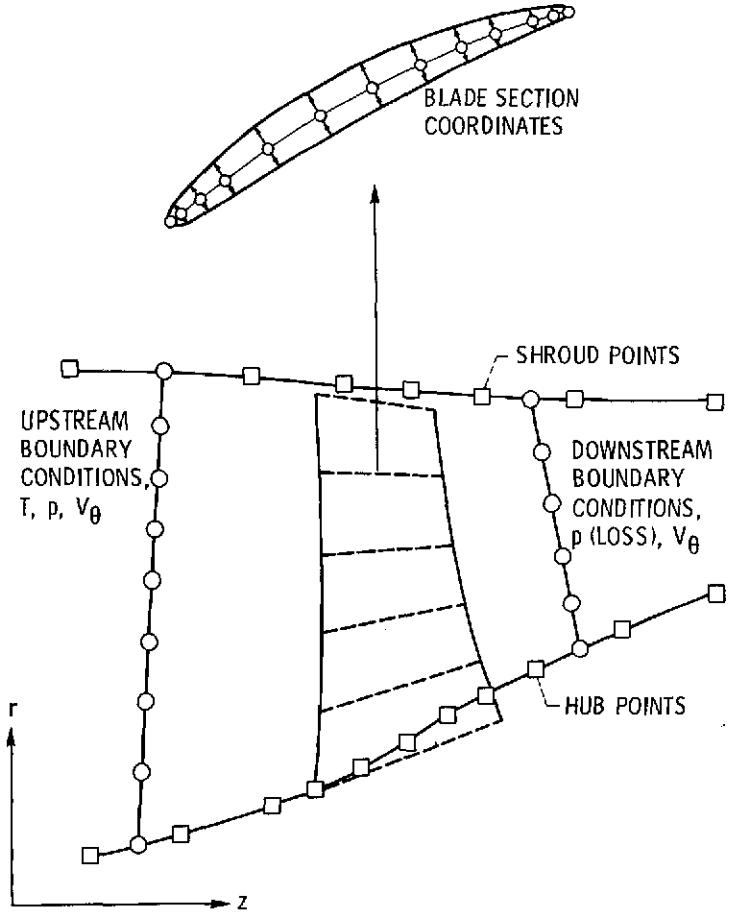

Figure 5. - MERIDL program input.

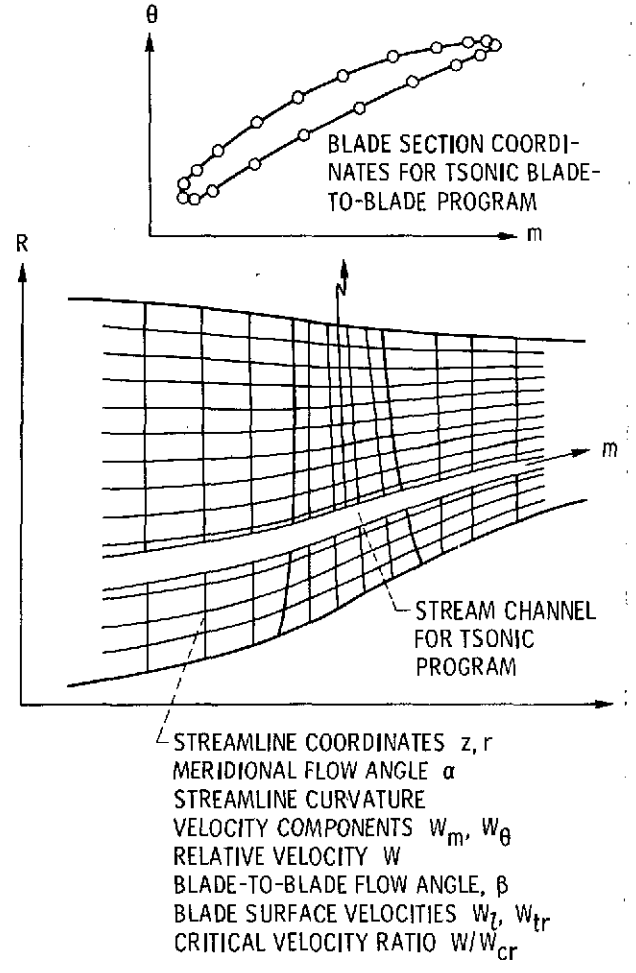

Figure 6. - MERIDL program output.

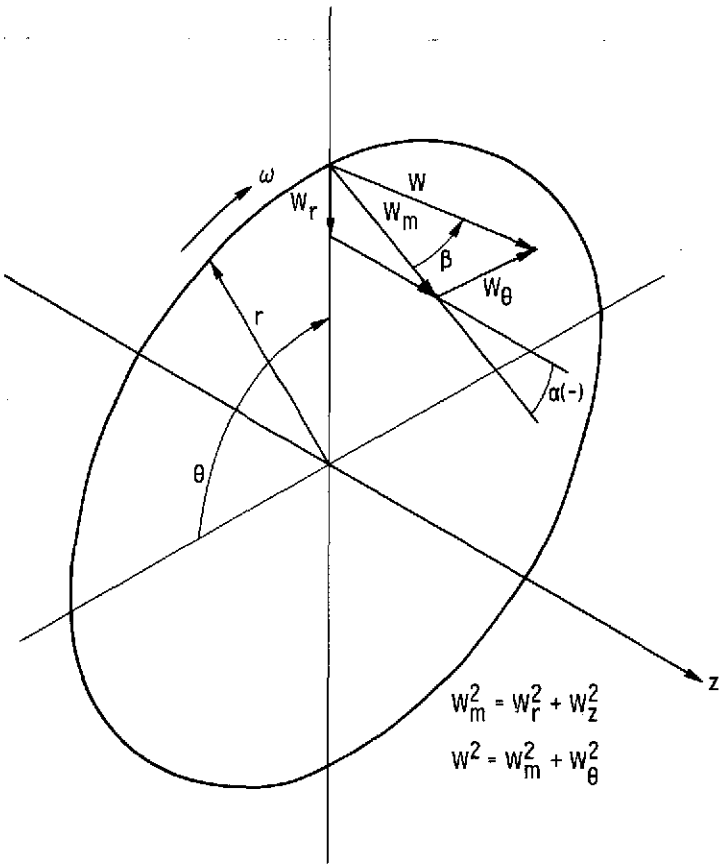

Figure 7. - Cylindrical coordinate system and velocity components.

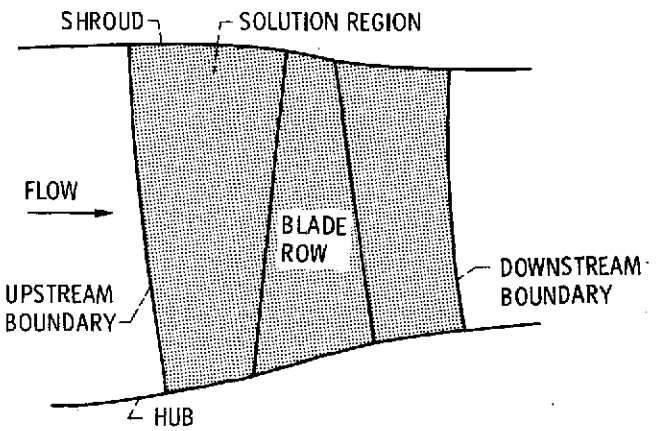

Figure 8. - Mid-channel surface solution region.

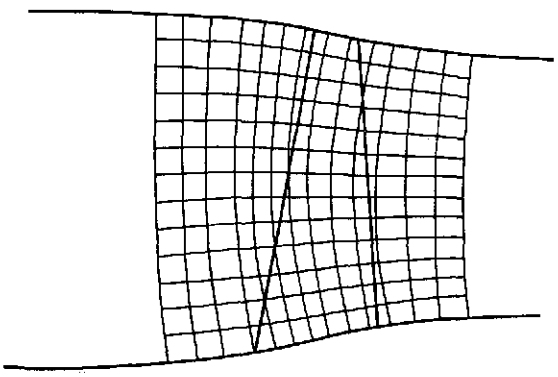

Figure 9. - Orthogonal mesh on the solution region.

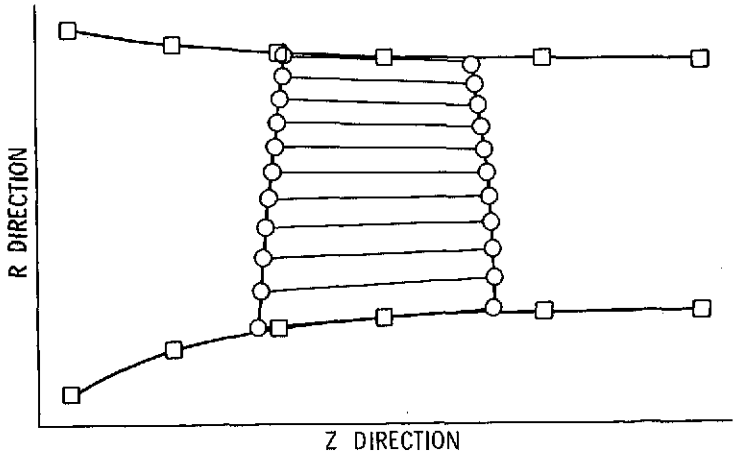

Figure 10. - Axial flow compressor rotor with design blade sections.

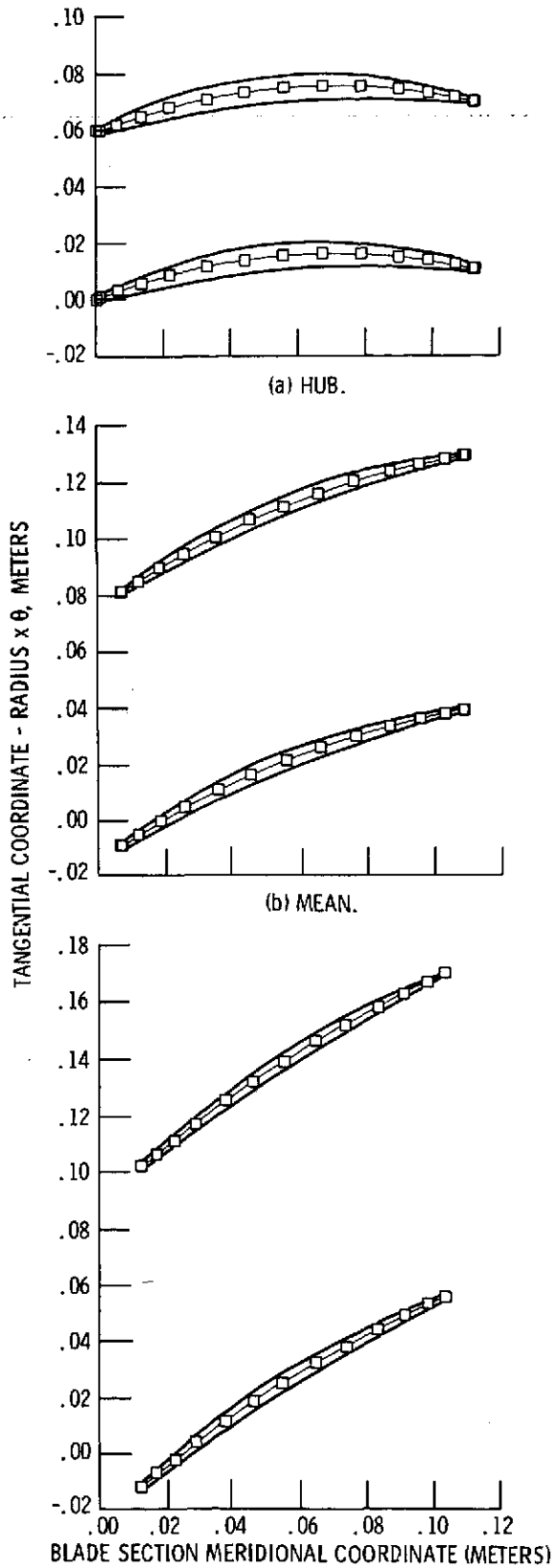

Figure 11. - Compressor rotor blade section.

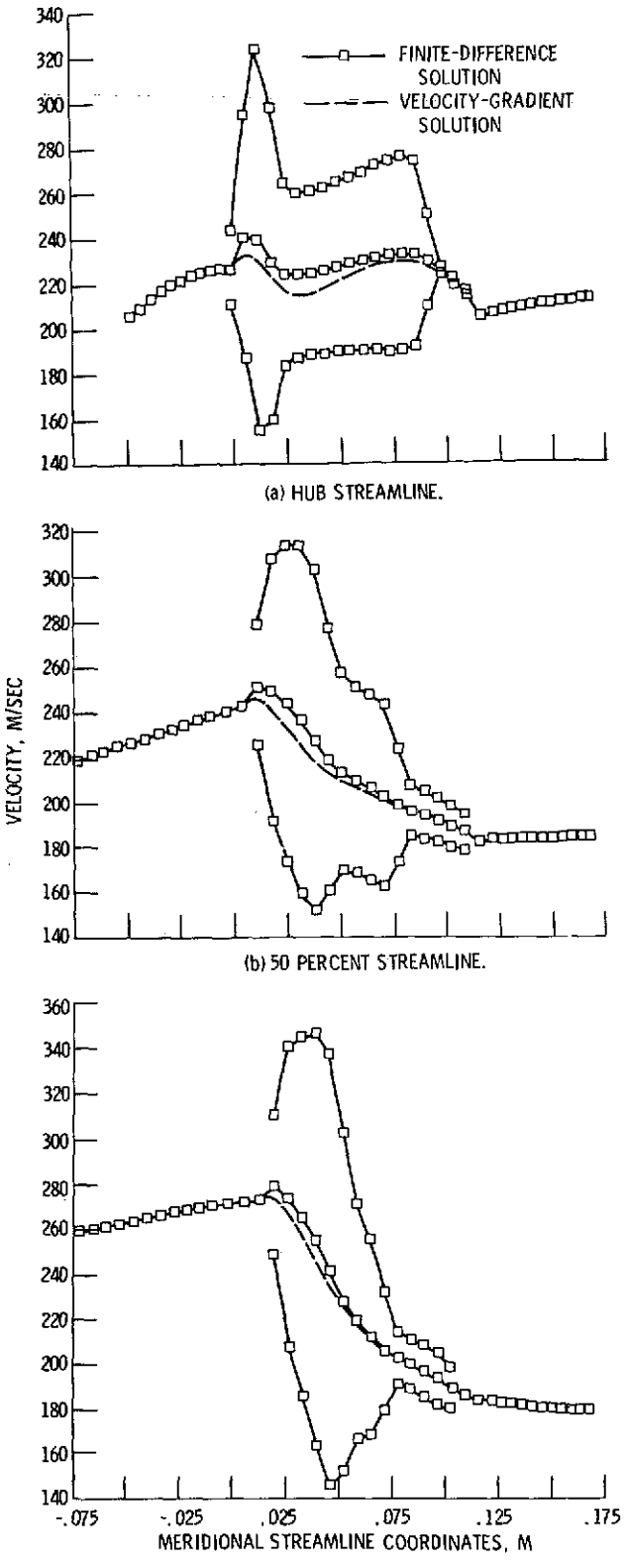

(a) HUB STREAMLINE.

(b) 50 PERCENT STREAMLINE.

(c) SHROUD STREAMLINE.

Figure 12. - Meridional and blade surface velocities for compressor rotor.

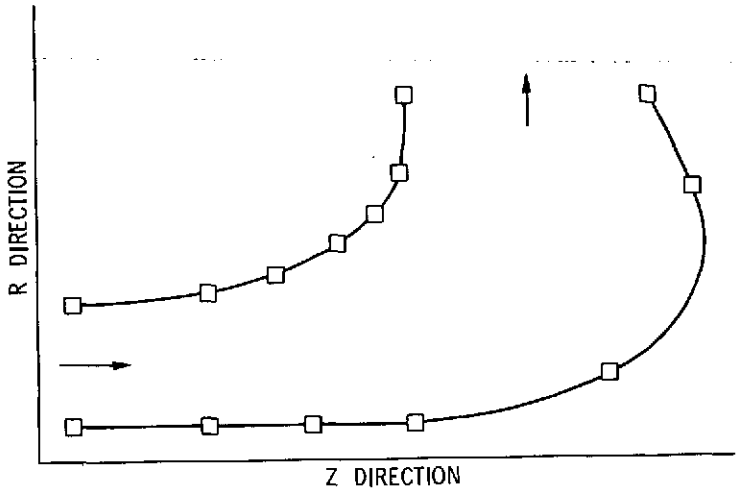

Figure 13. - Axial-to-radial diffuser duct.

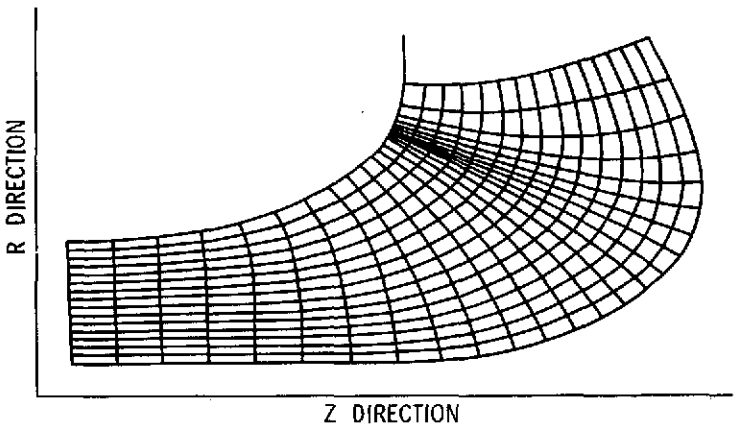

Figure 14. - Solution orthogonal mesh for diffuser duct.

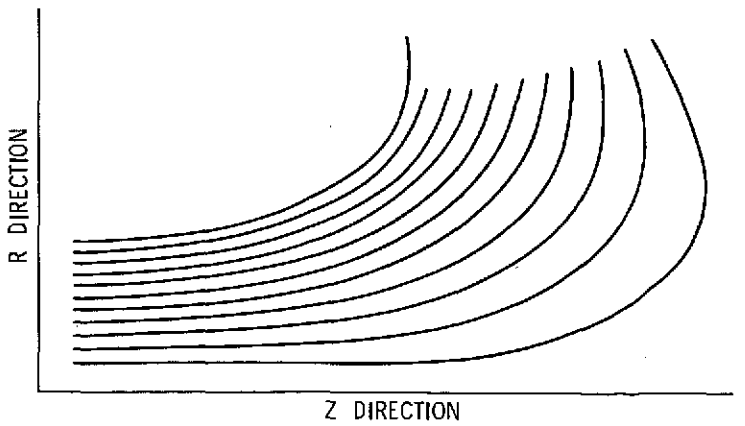

Figure 15. - Streamline plot for diffuser duct.

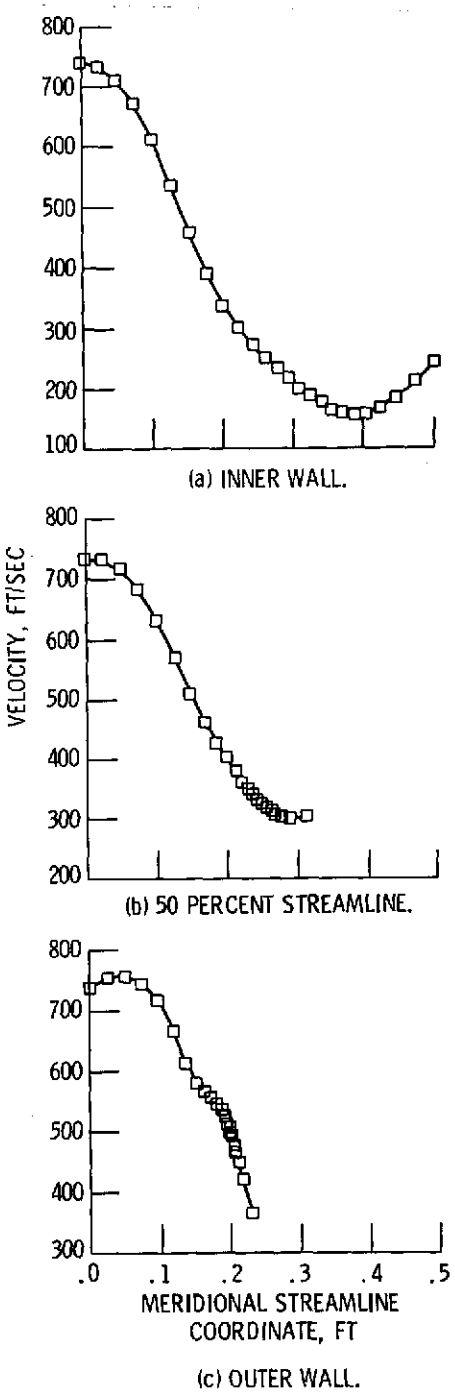

Figure 16. - Velocity distribution for diffuser duct.

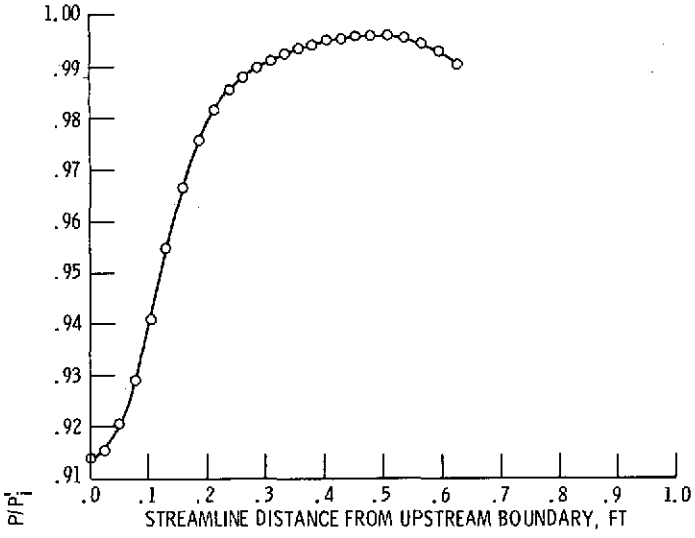

(a) INNER WALL STREAMLINE.

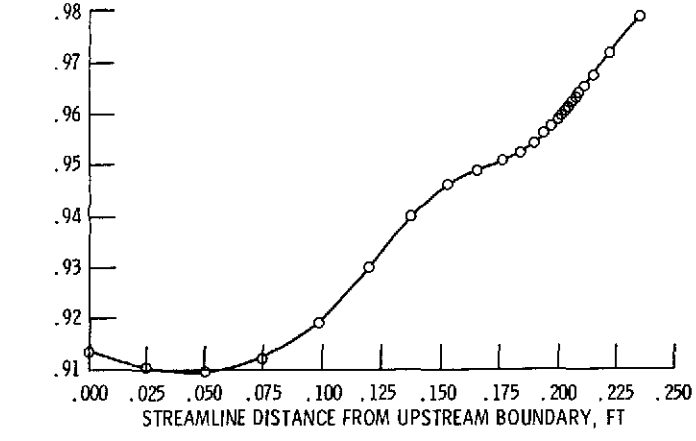

(b) OUTER WALL STREAMLINE.

Figure 17. - Static pressure distribution for diffuser duct.

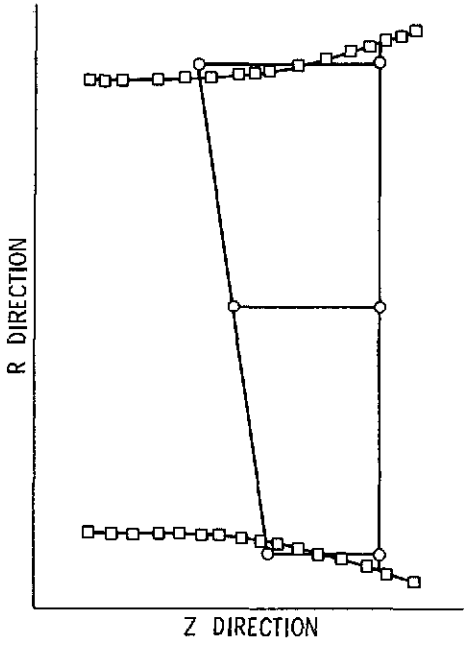

Figure 18. - Flared axial stator.

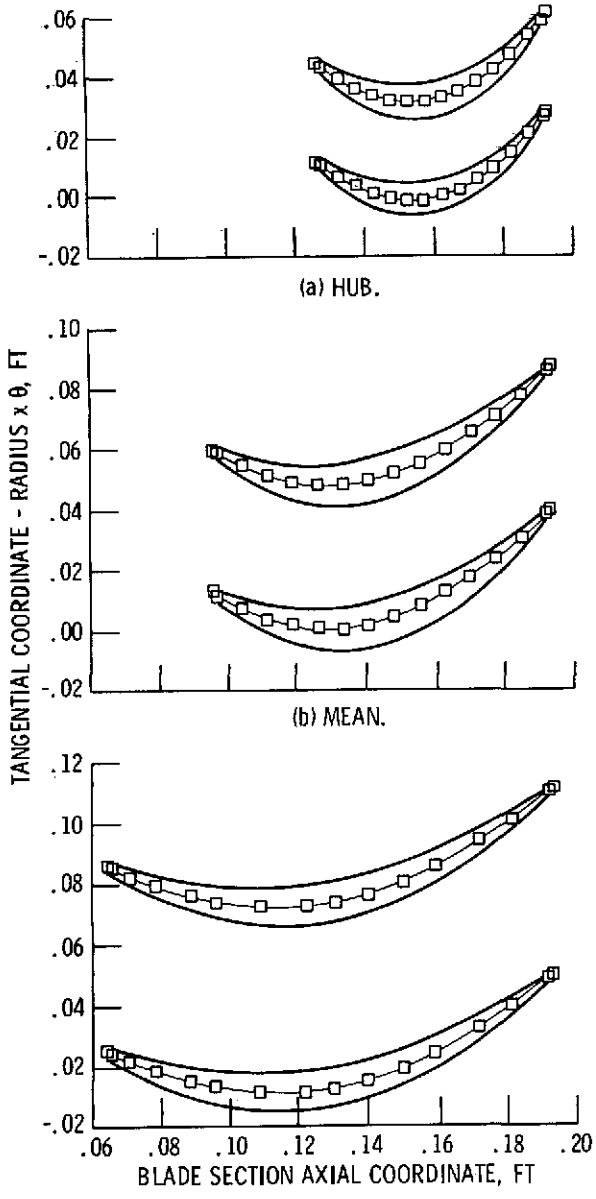

Figure 19. - Axial stator blade sections.

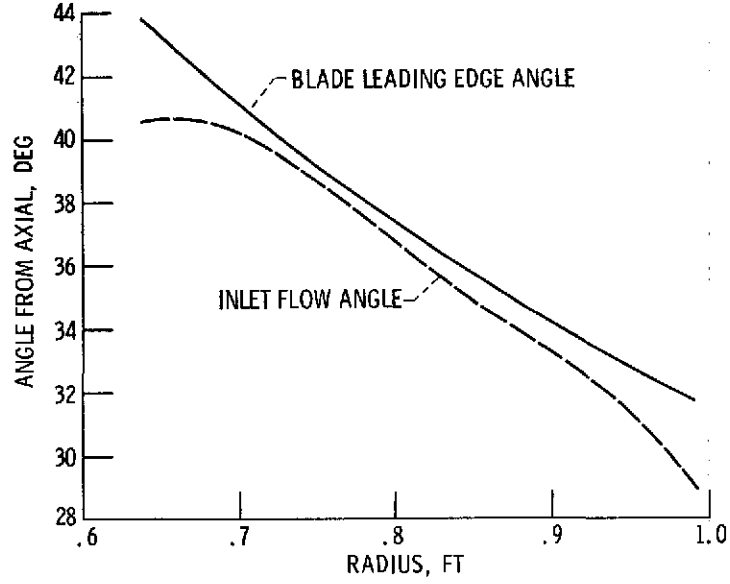

Figure 20. - Inlet flow angle compared with blade angle for axial flow stator.